



# Vacuum evaporated thin films of mixed cobalt and nickel oxides as electrocatalyst for oxygen evolution and reduction

V. Rashkova<sup>a,1</sup>, S. Kitova<sup>1a</sup>, I. Konstantinov<sup>1a</sup>, T. Vitanov<sup>b,\*</sup>

<sup>a</sup> Central Laboratory of Photoprocesses 'Acad. J. Malinowski', Bulgarian Academy of Sciences, Acad. G.Bonchev str., bl.109, Sofia 1113, Bulgaria

<sup>b</sup> Central Laboratory for Electrochemical Power Sources, Bulgarian Academy of Sciences, Acad. G.Bonchev str., bl.10, Sofia 1113, Bulgaria

Received 16 July 2001; received in revised form 12 December 2001

## Abstract

Mixed cobalt and nickel oxides, obtained by vacuum coevaporation of Co, Ni and TeO<sub>2</sub> are investigated as electrocatalysts for oxygen reduction and evolution reaction. Gas-diffusion bifunctional oxygen electrodes (GDE) are prepared by direct deposition of catalyst on gas-supplying membrane. Thus obtained GDE with different atomic ratio  $R_{\text{Co/Ni}}$  and  $R_{(\text{Co} + \text{Ni})/\text{Te}}$  of the catalyst are electrochemically tested by means of steady-state voltammetry. It is shown that the films exhibit high catalytic activity toward both oxygen reduction and evolution reactions despite very small catalyst loading of about 0.07 mg cm<sup>-2</sup>. © 2002 Elsevier Science Ltd. All rights reserved.

**Keywords:** Oxygen reduction; Oxygen evolution; Electrocatalysts; Cobalt and nickel oxides

## 1. Introduction

The search for highly efficient electrocatalysts for bifunctional oxygen electrode in metal–air and metal hydride–air rechargeable batteries remains an active area of research. It is well known that some transition metal oxides are the most promising electrocatalyst in alkaline solution [1–3]. NiCo<sub>2</sub>O<sub>4</sub>, has long been known to be an active bifunctional catalyst for oxygen evolution [3,4] and reduction in alkaline media [5,6], as well as a catalyst in alcohol and amine electro oxidation [7].

The electrocatalytic properties of metal oxides vary widely according to their method of preparation [8]. Different preparative methods might yield forms of NiCo<sub>2</sub>O<sub>4</sub> with differences in the bulk and in the surface structure, and with significantly different distributions

in the cation oxidation states. In the numerous investigations reported in the literature, the powder of oxides have been prepared by thermal decomposition of mixed nitrates, carbonates or hydroxides [3,4,8–10], sol–gel [8,11–13] or freeze drying method [14]. Thin films of NiCo<sub>2</sub>O<sub>4</sub> have been prepared by chemical spray pyrolysis [5] or by cathodic sputtering [15]. Ni–Co oxide electrodes have been prepared also by electrodeposition [16].

We have used a new method, described in detail elsewhere [17] for preparing mixed cobalt and nickel oxides by vacuum codeposition of TeO<sub>2</sub>, Co and Ni onto a substrate held at room temperature. It has been shown that during the vacuum deposition chemical interactions take place, resulting in oxide layers. Upon subsequent thermal treatment, the chemical reactions continue until complete consuming of TeO<sub>2</sub> or metal and formation of mixed oxides [17].

In this study we report the first results of the electrocatalytic activity investigations of thus vacuum-deposited catalyst of mixed oxides for both oxygen reduction and evolution reactions.

\* Corresponding author. Fax: +359-2-722-544.

E-mail addresses: rashkova@clf.bas.bg (V. Rashkova), skitova@clf.bas.bg (S. Kitova), konst@clf.bas.bg (I. Konstantinov), tvitanov@cleps.bas.bg (T. Vitanov).

<sup>1</sup> Fax: +359-2-722-465.

## 2. Experimental

### 2.1. Preparation of the catalyst and gas-diffusion electrodes

The mixed oxides were prepared by thermal coevaporation of Co by electron gun and  $\text{TeO}_2$  and Ni from independently heated cells of Knudsen type under vacuum better than  $10^{-4}$  Pa. The evaporation of  $\text{TeO}_2$  was carried out from Pt crucible, while those of Co and of Ni—from glassy carbon ones. The condensation rates of each substance within the range  $0.01\text{--}0.04\text{ }\mu\text{g cm}^{-2}\text{ s}^{-1}$  were controlled separately during the evaporation by quartz crystal monitor.

The substances were deposited on a stationary substrate, placed parallel to the emitting surfaces. In most of the cases a gas-diffusion membrane (GDM) was used as a substrate. The membrane consists of teflonized carbon blacks (45% teflon and 55% carbon blacks), hot pressed on Ni-screen [18]. For the transmission electron microscopy study however, air-cleaved mica with a carbon film on it was used as substrate.

The system of the mixed oxides condensed on the GDM represents the gas-diffusion electrode (GDE), the oxide being the active layer, while the membrane with Ni-screen as current collector inside—the gas-supplying layer of the electrode. The geometric area of GDE was

$1.5\text{ cm}^2$ . The GDEs were heated for 1 h at  $300\text{ }^\circ\text{C}$  in air for completing the oxidation of Co and Ni.

### 2.2. Characterization of the catalyst

The amount of each condensed substance and the atomic ratios  $R_{\text{Co/Ni}}$ ,  $R_{(\text{Co}+\text{Ni})/\text{Te}}$  at each point of the substrate were calculated from the crystal monitors data [19]. The chemical composition of the catalyst, deposited on GDM was controlled with an X-ray microanalyzer by scanning electron microscope (JEOL Superprobe 733 with mounted System 5000-HNU).

Scanning Electron Microscopy (Philips 515) as well as bright and dark field transmission electron microscopy and microdiffraction (JEOL 7) were applied for examining the morphology and structure of the catalyst. The chemical states of the elements in the catalyst film, deposited on the GDM were studied with X-ray photoelectron spectroscopy (XPS). The measurements were carried out in UHV chamber of the electron spectrometer ESCALAB MkII. The spectra were excited with an  $\text{MgK}\alpha$  source with energy  $1253.6\text{ eV}$ . The photoelectron lines of  $\text{C1s}$ ,  $\text{O1s}$ ,  $\text{Te3d}$ ,  $\text{Co2p}$  and  $\text{Ni2p}$  were recorded. All spectra were calibrated using  $\text{C1s}$  line at  $285.0\text{ eV}$  as a reference.

### 2.3. Electrochemical measurements

The electrochemical study was carried out by means of steady-state galvanostatic voltammetry using equipment consisting of potentiostat—galvanostat provided with a pulse generator (Solartron 1286 electrochemical interface).

The GDE were tested in a three-electrode cell at room temperature (r.t.). The electrolyte was 20% KOH, prepared with twice distilled water. Ni-plate was used as counter electrode. The potential was measured versus  $\text{Hg-HgO}$  reference electrode in 20% KOH, reaching close to test electrode by a Luggin capillary. The potentials were converted to the RHE (Real Hydrogen Electrode in the working electrolyte) scale using tabulated activity coefficient.

## 3. Results and discussion

In the present paper, we have studied GDE with two different compositions of the catalyst, given in Table 1. The results were obtained for catalyst loading of about  $0.07\text{ mg cm}^{-2}$ .

TEM examination of the catalysts, annealed at  $300\text{ }^\circ\text{C}$  under air atmosphere does not indicate the presence of crystalline phases, independent of the film composition. The electron diffraction pattern given in Fig. 1 shows that the catalyst film studied is amorphous.

Table 1  
Composition of the catalytic films and Tafel slopes of GDE

No. of sample	$R_{\text{Co/Ni}}$	$R_{(\text{Co}+\text{Ni})/\text{Te}}$	$b$ (mV per decade)	
			Oxygen reduction	Oxygen evolution
GDE1	4.5	0.78	66	128
GDE2	1.8	0.54	59	50

$R$ , atomic ratio.

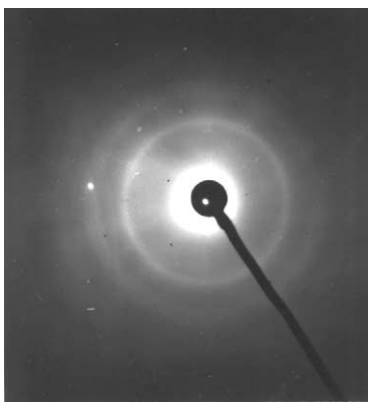


Fig. 1. Electron diffraction pattern of the catalytic film with composition 1.

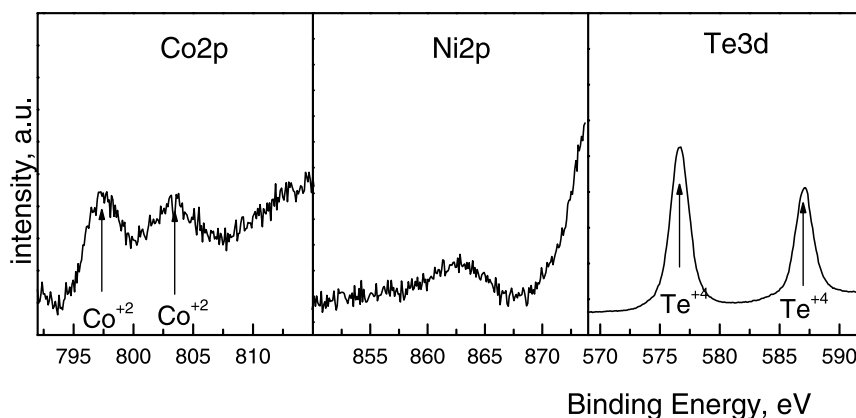
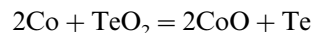


Fig. 2. Co2p, Ni2p and Te3d XPS spectra of GDE1.

The surface characterization of the degree of oxidation of the catalyst deposited on the GDM is made by XPS. Fig. 2 shows Co2p, Ni2p and Te3d spectra obtained for catalyst with composition 1 (GDE1 in Table 1). It should be noted that the similar XPS spectra are obtained for film with composition 2 (GDE2). The Co2p spectrum shows typical  $\text{Co}^{2+}$  state. The 2nd peak, which is at higher binding energy, is known to be shake-up satellite, which is exclusively observed in CoO [20,21]. Therefore, we believe that CoO phase dominates on the surface of the films studied. Our more detailed investigations show that the amount of  $\text{Co}^{2+}$  remains unchanged in the volume of the film. The elemental Co is not detected in the entire volume, which means that the whole amount of deposited Co is oxidized to  $\text{Co}^{2+}$ . The Ni2p spectrum, given in Fig. 2, does not indicate the presence of  $\text{Ni}^{2+}$  on the surface of the film, but  $\text{Ni}^{2+}$  was detected in the volume after slight  $\text{Ar}^+$  etching of the film. Fig. 2 indicates the presence of only  $\text{Te}^{4+}$  on the surface of the catalyst.  $\text{Te}^0$  signals are detected, however, in the volume of the film. It was found that the amount of  $\text{Te}^0$  increases and that of  $\text{Te}^{4+}$  decreases with the time of  $\text{Ar}^+$  etching. Most probably, oxidation of elemental Te proceeds on the surface of the film upon the thermal annealing in air. The presence of only  $\text{Co}^{2+}$  state as well as of  $\text{Ni}^{2+}$  state and elemental Te in the volume of the films studied confirms that the reactions



take place during the codeposition of Co, Ni and  $\text{TeO}_2$ . This gives us reason to consider that the catalyst films obtained are a mixture of cobalt, nickel and tellurium oxides.

Fig. 3 shows SEM micrographs of the GDM and the catalyst films with composition 1, deposited on the membrane (GDE1). It is seen that GDM as well as the catalyst film deposited on it have very large surface

areas. The film with composition 2 (GDE2) has a very similar surface. The small amount of catalyst deposited, of about  $0.07 \text{ mg cm}^{-2}$  has not completely covered the membrane surface. Therefore, it can be expected that the electrolyte will be in contact with both catalyst and carbon surface area. As it will be seen below (Fig. 4) the carbon is also active with respect to both oxygen evolution and reduction. To eliminate its influence, we have assumed that a measure of the catalytic activity of the evaporated catalyst is a difference of the current densities at a constant potential of covered by catalyst,

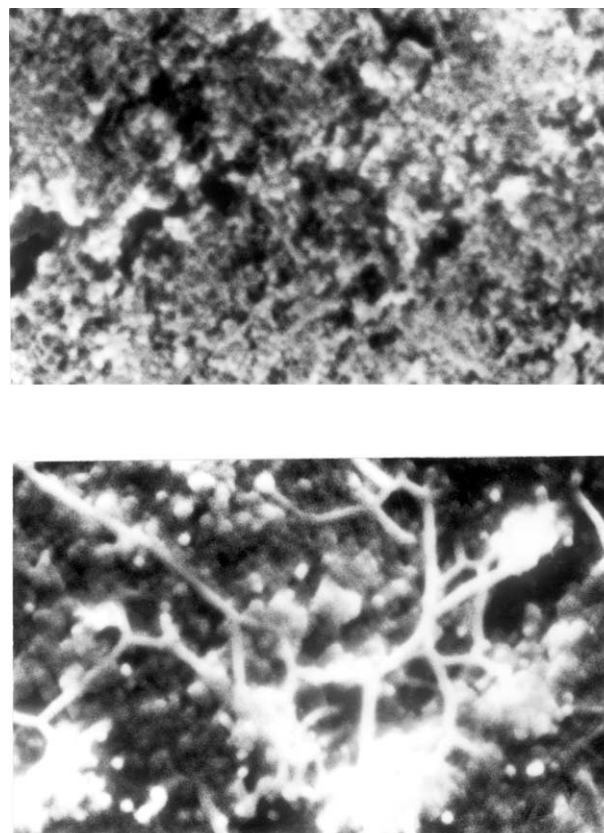


Fig. 3. SEM micrograph of GDM (a) and GDE1 (b).

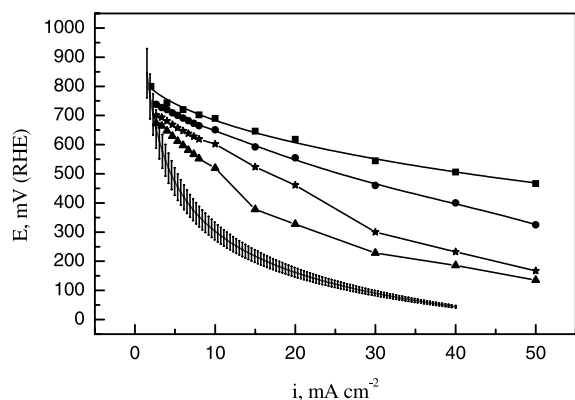


Fig. 4. Cathodic polarization curves of the GDEs in 20% KOH, measured in oxygen atmosphere: ■, GDE1; ●, GDE2; ★, TeO<sub>2</sub> film on GDM; ▲, Te film on GDM; ◆, average curve for GDMs, measured in oxygen atmosphere.

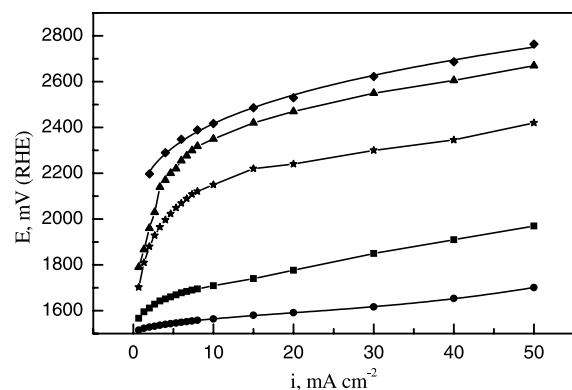


Fig. 5. Anodic polarization curves of the GDEs in 20% KOH: ■, GDE1; ●, GDE2; ★, TeO<sub>2</sub> film on GDM; ▲, Te film on GDM; ◆, GDM.

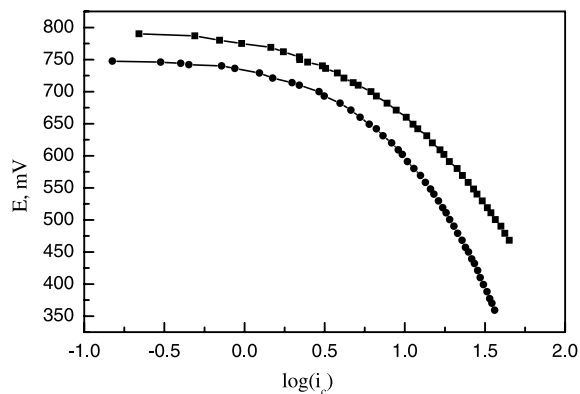


Fig. 6. Tafel plots of GDEs for oxygen reduction reaction: ■, GDE1; ●, GDE2.

$i_{mc}$  and free,  $i_m$ , GDM,  $i_c = i_{mc} - i_m$ . For finding  $i_c$  obviously, it is necessary to obtain reproducible  $E-i_m$  curves for the entire membrane.

Fig. 4 illustrates the current–voltage characteristics for oxygen reduction of GDEs with two different com-

positions of catalyst carried out in oxygen atmosphere. For comparison the curve of GDM without catalyst is given. The curve is averaged from measurement in oxygen atmosphere of four membranes and the bars show maximum deflections. It is seen the great increase of the current density in presence of catalyst, i.e. its significant catalytic effect for oxygen reduction.

The polarization curves for oxygen evolution of the same GDE compared with that of the membrane are given in Fig. 5. As seen, the oxides have high catalytic activity for oxygen evolution reaction.  $E-i$  curves of membranes covered with catalyst lie at significantly lower potentials in the whole range of current densities investigated, than the curve of membrane without catalyst. That is why we might consider that  $i_m = 0$ . Therefore,  $i_{mc} = i_c$  for oxygen evolution reaction and the values, obtained for GDE can be used as a measure of the catalyst activity.

As far as the catalytic activity of mixed Co and Ni oxides in oxygen reduction and evolution is well known, the question arises: what is the role of Te in these reactions? Figs. 4 and 5 show that TeO<sub>2</sub> and Te themselves exhibit some activity, which is significantly lower, especially for Te, than that of the catalyst.

Comparing Figs. 4 and 5 it can be seen, that GDE with higher catalytic activity for oxygen reduction reaction exhibits lower activity for oxygen evolution reaction and vice versa. The higher activity of the electrode Ni rich versus Co (Co/Ni = 1.8) in oer agrees with the literature data [3,22], while its lower activity in orr than that of the electrode rich in Co versus Ni (Co/Ni = 4.5) is in contradiction with [10]. The differences in catalytic activity obtained for the two compositions can be due to the different nature, as well as number and energy of the active centers. This results in different charge transfer limitations and/or transport hindrances of the reacting reagents and products of reaction in areas close to catalytic centers at higher current densities.

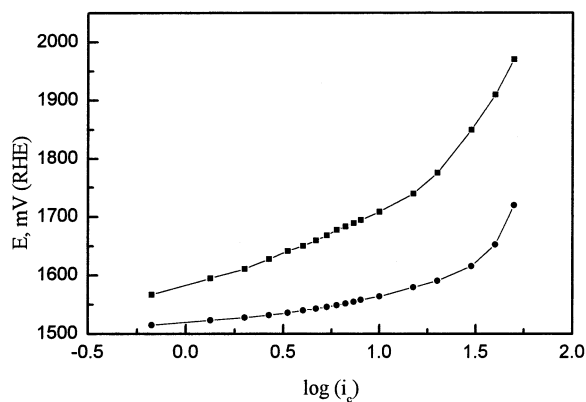


Fig. 7. Tafel plots of GDEs for oxygen evolution reaction: ■, GDE1; ●, GDE2.

Table 2  
Electrode activity for oxygen reduction and evolution

Electrode	Loading (mg cm <sup>-2</sup> )	$i$ (mA) cm <sup>-2</sup> at $E$ (mV) vs. RHE			
		700		1600	
		$i_{app}$ (mA cm <sup>-2</sup> )	$i_m$ (mA mg cm <sup>-2</sup> )	$i_{app}$ (mA cm <sup>-2</sup> )	$i_m$ (mA mg cm <sup>-2</sup> )
NiCo <sub>2</sub> O <sub>4</sub> (sol-gel [22])	2.8	–	–	324	115
NiO-CoO (low temperature [23])	14	25	1.8	38	2.7
Co-Ni-Te-O	0.07	10	143	23	328

In Figs. 6 and 7 are depicted the Tafel plots for GDE1 and 2. The values of Tafel slopes  $b$ , obtained for the both reactions are given in Table 1. The same value of  $b \sim 60$  mV per decade for oxygen reduction is an indication for identical reaction mechanism for both electrodes.

Completely different values for the Tafel slope  $b$  are obtained, however, for oxygen evolution ( $\sim 50$  mV per decade for GDE2 and  $\sim 128$  mV per decade for GDE1). The higher value of  $b$ , obtained for GDE1 is due most probably to the different mechanism of the anodic reaction. At this stage, it is difficult to explain the processes, leading to different Tafel slopes for oxygen evolution reaction, as well as the mechanism of oxygen reduction reaction.

It is interesting to compare the electrocatalytic activity of the oxides studied with that of oxides prepared by other methods. As far the apparent current density depends on the catalyst loading more informative would be the comparison of both the apparent (mA cm<sup>-2</sup>) and mass activity (mA cm<sup>-2</sup> g<sup>-1</sup>). Because of the lack of literature data for catalyst loading, the comparison in Table 2 is made only with two oxides, prepared by sol-gel [22] and low temperature technique [23]. The data presented show that GDE with high mass activity as well as high apparent activity (mA cm<sup>-2</sup>) can be developed by the method described. To achieve this, the optimization of the active films with respect to the catalyst loading, the composition, as well as the evaporation conditions and post-annealing is necessary.

#### 4. Conclusion

Amorphous electrocatalyst of mixed cobalt, nickel and tellurium oxides, obtained by vacuum codeposition of TeO<sub>2</sub>, Co and Ni can be used for preparing electrodes for both the oxygen evolution and reduction reactions. During vacuum deposition, the coevaporated compounds are mixed at atomic level. This gives a possibility to obtain catalyst with various components in desired proportions. Another advantage of this method is the opportunity to obtain electrodes with

very high surface-volume ratio. Thus obtained GDEs have high catalytic activity for oxygen evolution and reduction reactions with very small catalyst loading of approximately 0.07 mg cm<sup>-2</sup>.

#### Acknowledgements

The authors are grateful to Dr K. Petrov, who participated in the beginning of this study, and for his helpful advice and comments.

#### References

- [1] M.R. Tarasevich, B.N. Efremov, in: S. Trasatti (Ed.), *Electrodes of Conductive Metallic Oxides*, Part A, Elsevier, Amsterdam, 1980, p. 221.
- [2] A.C.C. Tseung, K.L.K. Jeung, *J. Electrochem. Soc.* 125 (1978) 1003 and the literature there in.
- [3] I. Nicolov, R. Darkaoui, E. Zhecheva, R. Stoyanova, N. Dimitrov, T. Vitanov, *J. Electroanal. Chem.* 429 (1997) 157.
- [4] J. Haenen, W. Visscher, E. Barendrecht, *J. Electroanal. Chem.* 208 (1986) 273.
- [5] R.N. Singh, J.F. Koenig, G. Poillerat, P. Chartier, *J. Electroanal. Chem.* 314 (1991) 241.
- [6] N. Heller-Ling, M. Prestat, J.L. Gautier, J.F. Koenig, G. Poillerat, P. Chartier, *Electrochim. Acta* 42 (1997) 197.
- [7] E. Hayes, B. Bellingham, H. Mark Jr., Galal Ahmed, *Electrochim. Acta* 41 (1996) 337.
- [8] J. Marco, J. Gancedo, M. Gracia, J. Gautier, E. Rios, F. Berry, *J. Solid State Chem.* 153 (2000) 74.
- [9] H. Carapuca, M. Pereira, F. Costa, *Mat. Res. Bull.* 25 (1990) 1183.
- [10] W. King, A. Tseung, *Electrochim. Acta* 19 (1974) 485.
- [11] F. Svegli, B. Orel, M.G. Hutchins, K. Kalcher, *J. Electrochem. Soc.* 143 (1996) 1532.
- [12] M.L. Baydi, M.G. Poillerat, J.L. Gautier, J.L. Rehspringer, J.F. Koenig, P. Chartier, *J. Solid State Chem.* 109 (1994) 278.
- [13] M.L. Baydi, S.K. Tiwari, R.N. Singh, J.L. Rehspringer, P. Chartier, J.F. Koenig, M.G. Poillerat, *J. Solid State Chem.* 116 (1995) 157.
- [14] P. Rasiyah, A. Tseung, *J. Electrochem. Soc.* 130 (1983) 2384.
- [15] B. Nkeng, G. Poillerat, J. Koenig, P. Chartier, B. Lefez, J. Lopitiaux, M. Lenglet, *J. Electrochem. Soc.* 142 (1995) 1777.
- [16] E. Castro, C. Gervasi, J. Vilche, *J. Appl. Electrochem.* 28 (1998) 835.
- [17] S. Kitova, V. Rashkova, I. Konstantinov, Vacuum, in press.
- [18] T. Vitanov, I. Nikolov, K. Petrov, E. Zecheva, R. Stoyanova, Bulg. Patent, 101585/06.06.1997.

- [19] I. Podolesheva, P. Gushterova, V. Platicanova, I. Konstantinov, *J. Vac. Sci. Technol., A* 16 (1997) 674.
- [20] M. Tanaka, M. Mukai, Y. Fujimori, M. Kondoh, Y. Tasaka, H. Baba, S. Usami, *Thin Solid Films* 281–282 (1996) 453.
- [21] J. Kim, D. Pugmire, D. Battaglia, M. Landell, *Appl. Surf. Sci.* 165 (2000) 70.
- [22] R. Singh, J. Pandey, N. Singh, B. Lal, P. Chartier, J. Koenig, poster presented at the Symposium Electrochemistry and Materials: Synthesis and Characterization, 50th ISE Meeting, Pavia, Italy, September 1999, pp. 5–10.
- [23] S. Gamburgzev, W. Zhang, O.A. Velev, S. Srinivasan, A.J. Appleby, A. Visintin, *J. Appl. Electrochem.* 28 (1998) 545.